A Mesoscale Model for EM Ducting in the Marine Boundary Layer

Martin J. Otte,* Nelson L. Seaman, David R. Stauffer, and John C. Wyngaard

The Pennsylvania State University
University Park, Pennsylvania

1. Introduction

Meteorological processes within the marine boundary layer (MBL) play an important role in determining EM propagation conditions. The profiles of temperature and humidity in the atmosphere determine the refractivity conditions. Often, these profiles can lead to anomalous propagation mechanisms within the MBL. Examples of these nonstandard propagation mechanisms include evaporation ducts where the specific humidity of water vapor decreases rapidly just above the sea surface, and elevated trapping layers caused by the simultaneous rapid increase in temperature and decrease in water vapor within the inversion which typically caps the MBL.

Advances in numerical weather prediction methods, coupled with increased computing power, are now allowing for improved forecasts of refractivity conditions on the mesoscale. Mesoscale weather prediction models can provide three-dimensional, time-dependent forecasts of refractivity on horizontal scales of about 10 km over a total area of over 50,000 km^2. Burk and Thompson (1995) demonstrate the validity of mesoscale model forecasts of refractivity using the Navy Operational Regional Atmospheric Prediction System (NORAPS). They found that the mesoscale forecasts performed well in describing the general refractivity conditions observed during the Variability of Coastal Atmospheric Refractivity (VOCAR) experiment which was conducted off the coast of California between Pt. Conception and San Diego.

However, Burk and Thompson note that the model did not behave as well in predicting trapping layers and ducting events. There are three basic shortcomings of mesoscale models which we have identified that need to be addressed for them to be useful for propagation assessment:

1) Proper model initialization. Mesoscale models typically use a combination of global forecast model fields and observed conditions for initialization. Unfortunately, the MBL is often not represented well in coarse global models, and there is a tremendous lack of meteorological observations over the ocean. The proper temperature and moisture fields, which determine the propagation environment, generally will be absent in mesoscale initial conditions over the ocean. Leidner and St suffer (1996) correct for this deficiency by using climatological data within the assimilation cycle of a mesoscale model with sufficient resolution to represent the MBL.

2) Improved model physics. Mesoscale models contain "submodels" which represent meteorological processes that the host mesoscale model cannot explicitly resolve. Examples of these processes include solar and longwave radiative fluxes, the influence of subgrid clouds, and marine boundary layer turbulence. For modelling the propagation environment, it is important that the MBL parameterizations within the mesoscale model provide realistic MBL structure. We are augmenting the MBL scheme within the mesoscale model to provide realistic profiles of temperature and humidity, including

* Corresponding *author* address: Martin J. Otte, 503 Walker Bldg., Department of Meteorology, University Park, PA 16801-5013. *Email:* otte@essc.psu.edu

the trapping layer height and structure.

3) Inclusion of turbulent structure. There are many meteorological processes that occur on scales smaller than the grid spacing of the mesoscale model. Khanna *et* al. (1997) show with a fine-scale numerical model the turbulent motions which exist in the atmosphere and are not represented by the mesoscale fields. It is known that these turbulent motions can have important influences on the refractivity field, and produce scattering of the EM waves. Gilbert *et al.* (1990) demonstrate the importance of the scattering contribution to propagating sound waves in the atmosphere. These subgrid effects must be considered for mesoscale refractivity forecasts to be complete.

The Penn State University/National Center for Atmospheric Research (PSU/NCAR) mesoscale model MM5 (Grell *et* al.) is being used to determine the validity of using mesoscale models to forecast the propagation environment. The model is being augmented to correct for the deficiencies noted above. A description of the necessary improvements to the mesoscale model follows.

2. Marine Boundary Layer Initialization

The MM5 mesoscale model is initialized using Four-Dimensional Data Assimilation (FDDA). With FDDA, analysis or individual observations are assimilated into the model fields during a pre-forecast assimilation period (Stauffer and Seaman, 1994). Observation nudging is typically used in data-sparse regions to assimilate data into the model. With these techniques, the model fields are nudged toward the observed values during the initialization period using a Newtonian nudging term in the governing equations.

With few data available to define the MBL in the initial conditions, this technique does not produce a realistic initial MBL. Leidner and Stauffer hypothesized that including climatological information in the assimilation cycle would produce improved MBL structure over ocean locations. Even though the climatological conditions would not be expected to describe the meteorology at a particular day, they provide statistically significant input which, when combined with the model equations, produces a better initial state. The climatology of Neiburger *et* al. (1961) is used to characterize the northeast Pacific Ocean during summer.

Fig. 1 shows a cross section of potential temperature and cloud water fields near Pt. Conception at the end of the initialization cycle. In Fig. la, no climatological information was assimilated, while Fig. lb includes the climatological assimilation. The climatological information allows for a much stronger inversion, which slopes upward towards the west. Leidner and Stauffer also note that the cloud field produced in Fig. lb agrees better with observations than Fig. 1a. The stronger, sloping inversion in Fig. lb also agrees better with observations, and would conceivably yield an improved refractivity environment. Fig. 2 shows the results after a 24 hr forecast using the results of the assimilation cycle shown in Fig. 1. The important point to note is that the model is able to retain the strong, sloping inversion through the forecast period, while this structure has not yet formed in the experiment without the climatological nudging.

3. Model Parameterizations

With improved model initialization, the next step is to improve the model physical parameterizations to ensure realistic profiles within the marine boundary layer. The three distinct regions of the MBL to be parameterized are the surface layer, the mixed layer, and the inversion layer. Each of these regions is shown in Fig. 3, along with a schematic of the mean profiles of potential temperature Θ, specific humidity q, and modified refractivity M typically found within the marine boundary layer. These regions typically produce an elevated trapping layer and surface-based duct within the MBL.

The surface layer occupies approximately the lowest 10% of the MBL adjacent to the sea surface. It is the region of the MBL which is the most studied. An evaporation duct often exists within the marine surface layer due to the rapid decrease of humidity with height just above the sea surface. The mean temperature and humid-

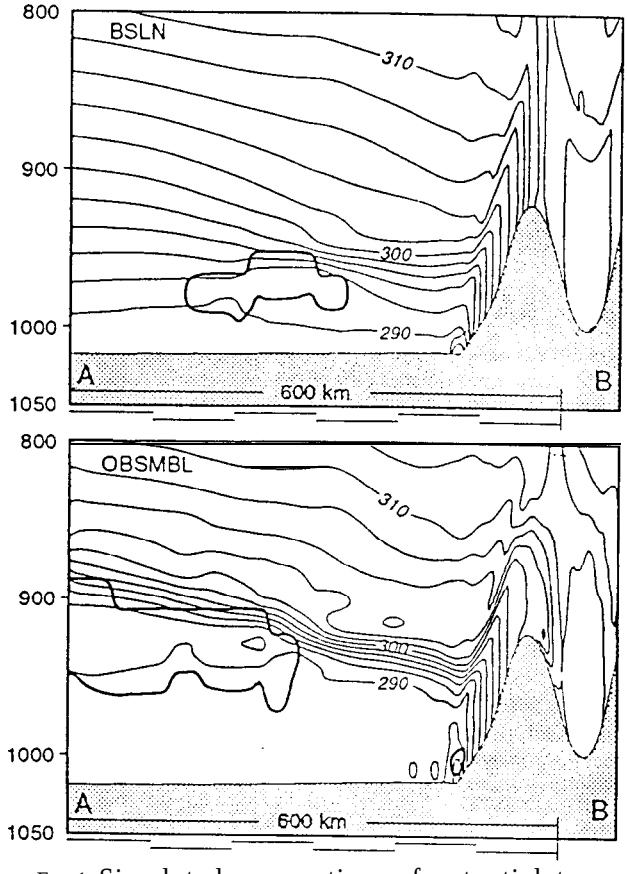

FIG. 1. Simulated cross sections of potential temperature (thin, every 2K) and cloud boundary at t=O (0000 UTC 4 August 1990) for (a) no climatological assimilation and (b) with climatological assimilation. After Leidner and Stauffer (1996).

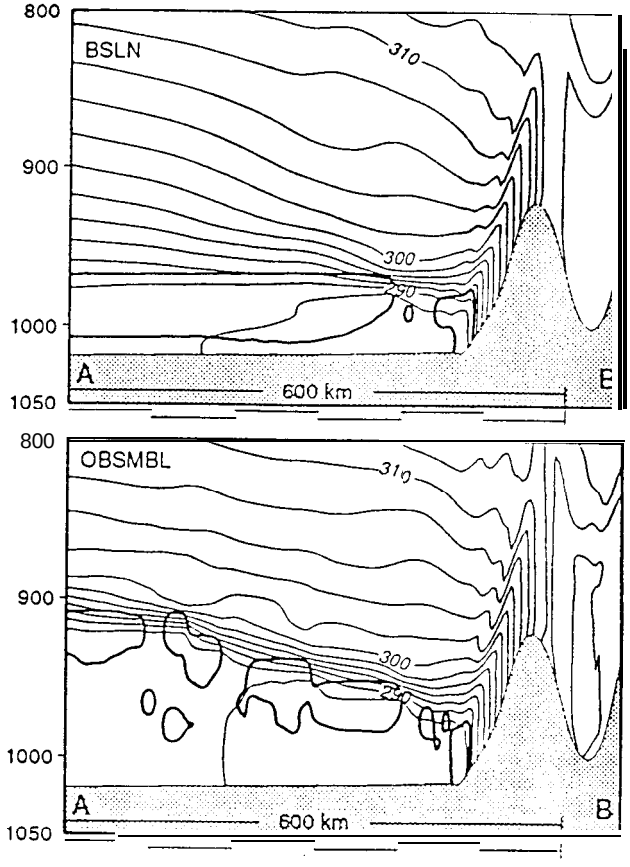

FIG. 2. Same as Fig.1, but at t=24 h

ity profiles within the surface layer can be modelled using Monin-Obukhov similarity as:

$$\Theta(z) = \Theta_s - \frac{\Theta_*}{k}\left(\ln\frac{z}{z_0} - \Psi_h\right) \qquad (1)$$

$$q(z) = q_s - \frac{q*}{k}\left(\ln\frac{z}{z_0} - \Psi_h\right) \qquad (2)$$

where Θ is the potential temperature and q the specific humidity of water vapor at height z, k is Von Karman's constant, Z. is the surface roughness length, Θ_* and q_* are scales for temperature and humidity, respectively, and Ψ_h is a stability-dependent correction to the neutral profile. Rogers and Paulus (1997a) give a good summary on how models based on Monin-Obukhov similarity are used to provide the re-

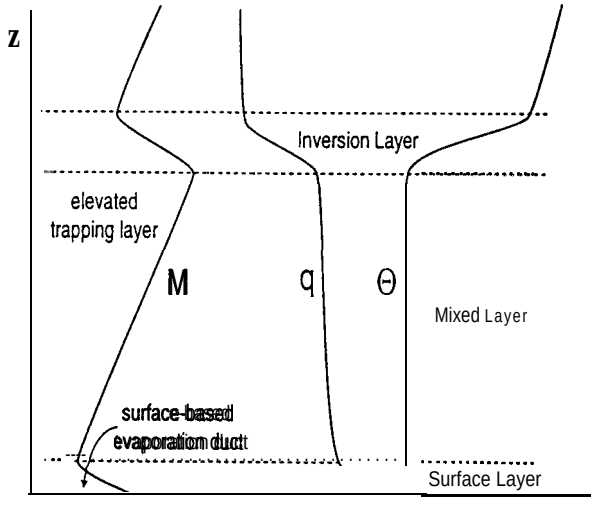

FIG. 3. An idealized schematic showing the three regions of the MBL along with typical mean profiles of potential temperature Θ, humidity q, and resulting modified refractivity M.

fractive conditions within the surface layer and predict evaporation ducts.

The mixed layer extends from just above the surface layer up to the inversion which caps the MBL. The mean profiles of potential temperature and humidity are often nearly well-mixed in this region due to the large turbulent eddies which exist within the mixed layer. The turbulent eddies get their energy from the mean shear, surface buoyancy forcing, and radiative cooling produced at the top of the stratocumulus clouds which often cap the MBL. We are currently looking at observations and fine-scale numerical modeling datasets to formulate a model of the marine mixed layer which will provide realistic mean temperature and humidity profiles.

Within the inversion region which caps the MBL, the potential temperature increases and the specific humidity decreases rapidly with height, often leading to elevated trapping layers and surface-based ducts. The important considerations for modeling this region include the height of this trapping layer, and the vertical gradients which exist there. Ignoring advection, the trapping layer depth h is determined from:

$$\frac{\partial h}{\partial t} = w - w_e \qquad (3)$$

where w is the large-scale vertical velocity produced by the mesoscale model, and we is the rate that the MBL turbulence is entraining air from above; w_e must be parameterized. Often, a fine balance exists between these two values, resulting in discrepancies in trapping layer depth between models. Again, we are looking at datasets from large-eddy simulation (LES) to parameterize the entrainment rate which determines the trapping layer depth and the mean gradients which exist there.

4. Subgrid Information

Even if the mesoscale model could produce perfect forecasts of the mean refractive conditions, there would still be problems in using the mesoscale profiles due to the subgrid meteorological effects which are not represented by the mesoscale model. Turbulence which is subgrid to the mesoscale model induces random perturbations on the large-scale refractive profiles produced by the mesoscale model. Fig. 4 shows the local refractive index structure function parameter $\tilde{C}_{N^2}$ obtained through LES by Khanna *et al.* (1997). Peltier and Wyngaard (1995) discuss the importance of this parameter to the scattering of transmitted waves by turbulence. This field represents a snap-shot of the squared intensity of refractivity n at inertial-range scales of motion.

It is clear from Fig. 4 that there is a large turbulent influence on the refractivity field near the inversion region at the top of the MBL. This is due to the undulations in the inversion caused by the MBL turbulence. These undulations in the inversion result in additional anamolous propagation and scattering of EM waves. Data from vertically pointing acoustic sounders also clearly show the strong turbulent scattering of waves due to the large perturbations in the refractivity field at the inversion.

Khanna *et al.* discuss large-eddy simulation and how it can help describe the propagation characteristics within the MBL. However, LES is not an operational tool to predict the propagation environment. With the large computing time needed to run LES, it is only used as a research tool to help us understand the structure of the MBL. LES is being used to develop datasets that will allow us to augment the fields produced by the mesoscale model to include the effects of turbulence on the refractivity environment.

5. Conclusions

Advances in mesoscale meteorological modeling and increased computing power are allowing for forecasts of refractive conditions within the MBL. However, there still are some improvements needed in mesoscale models for them -- to be applicable for propagation assessment. We identified problems with mesoscale model initialization, MBL physical parameterizations, and the influence of subgrid turbulence. We have begun to look at these problems, but they will only be solved by interaction between the mesoscale modeling, atmospheric turbulence, and EM propagation communities.

The data assimilation results show how using alternate forms of data over observation-sparse areas can result in improved initial conditions and model forecasts. Other forms of data which may be useful over ocean locations include propagation measurements (Rogers and Paulus, 1997b). Even wit h the inherent ambiguities in inverting propagation measurements to determine the atmospheric state, this data may still give statistically significant information which, when combined with the mesoscale model equations, produces better initial conditions and forecasts.

Acknowledgements. This work is supported by Navy contract No. NOOO39-92-C-O1OO, Task No. 07A-2015.

6. References

Burk, S. D., and W. T. Thompson, 1995: Mesoscale modeling of refractive conditions in a complex coastal environment. *Propagation Assessment in Coastal Environments,* AGARD Conf. Proc. 567, 40-1-40-6.

Gilbert, K. E., R. Raspert, and X. Di, 1990: Calculation of turbulence effects in an upward-refracting atmosphere. *J. Acoust. Sot. Am., 87, 2428-2437.*

Grell, G. A., J. Dudhia, and D. R. Stauffer, 1994: *A Description of the Fifth-Generation Penn State/NCAR Mesoscale* Model *(MM5).* NCAR Technical Note 398+STR, National Center for Atmospheric Research, Boulder, CO, 138 pp.

Khanna, S. and J. C. Wyngaard, 1997: Local refractive index structure-function parameter and its application to wave propagation. This volume.

Leidner, S. M., and D. R. Stauffer, 1996: Improving California coastal-zone forecasting by initialization of the marine boundary layer. *Preprints, 11th* Conference on *Numerical Weather Prediction, 177–179.*

Neiburger, M. D., D. Johnson, and C. Chien, 1961: *Studies of the Structure of the Atmosphere Over the Eastern Pacific Ocean in Summer: I Inversion Over the Eastern North Pacific Ocean,* Univ. Calif. Publ. Meteor., **1, No.** 1, 94 pp.

Peltier, L. J. and J. C. Wyngaard, 1995: Structure-function parameters in the convective boundary layer from large-eddy simulation. *J. Atmos. Sci., 52, 3641–3660.*

Rogers, L. T., and R. A. Paulus, 1997a: Measured performance of evaporation duct models. This volume.

Rogers, L. T., and R. A. Paulus, 1997b: Fusing data from the mesoscale model and radio remote sensing. This volume.

Stauffer, D. R. and N. L. Seaman, 1994: Multiscale four-dimensional data assimilation. *J. Appl. Meteo., 33, 416–434.*

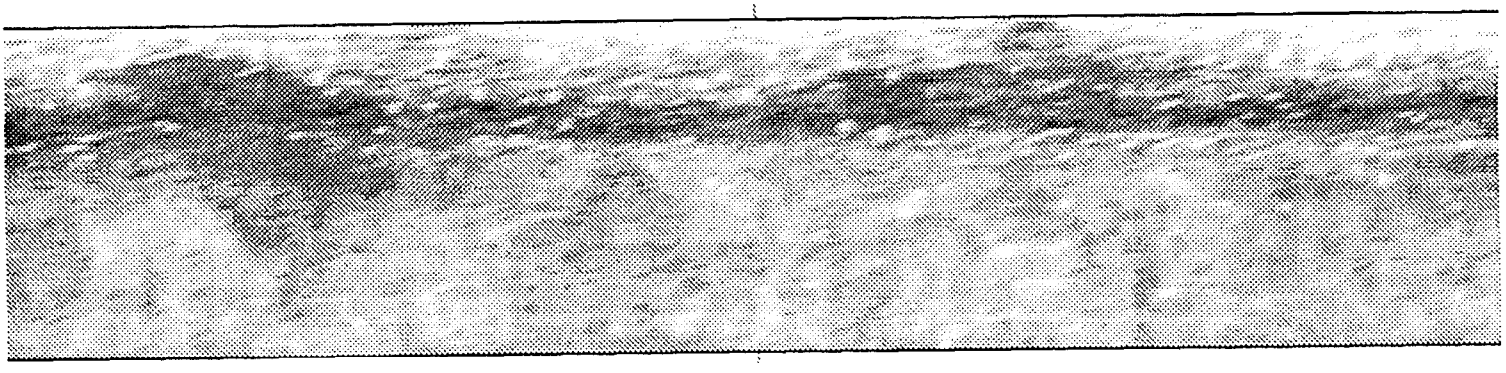

FIG. 4. .4 cross section of a large-eddy simulation of the MBL showing the local refractive index structure function parameter $\tilde{C}_{N^2}$. Dark regions denote high $\tilde{C}_{N^2}$ indicating large turbulent perturbations in the refractivity field at inertial-range scales. The model shows the largest $\tilde{C}_{N^2}$ near the top of the MBL at the inversion, which is caused by turbulent undulations in the inversion. The model domain is about 1 km in the vertical and 2 km in the horizontal